sensors

MDPI

Article

Artificial Intelligence ECG Analysis In Patients With Short QT Syndrome To Predict Life-Threatening Arrhythmic Events

Eros Pasero [1,*], Fiorenzo Gaita [2,3], Vincenzo Randazzo [1,*], Pierre Meynet [3,4], Sergio Cannata [1], Philippe Maury [5], and Carla Giustetto [3,4,*]

[1] Department of Electronics and Telecommunications, Politecnico di Torino, 10129 Turin, Italy
[2] Cardiology Unit, J Medical, Turin, Italy
[3] Department of Medical Sciences, University of Turin, Turin, Italy
[4] Division of Cardiology, Città della Salute e della Scienza Hospital, Turin, Italy
[5] University Hospital Rangueil, Cardiology, Toulouse, France
* Correspondence: eros.pasero@polito.it (E.P.); vincenzo.randazzo@polito.it (V.R.); carla.giustetto@unito.it (C.G.)

Abstract: Short QT syndrome (SQTS) is an inherited cardiac ion channel disease related to an increased risk of sudden cardiac death (SCD) in young and otherwise healthy individuals. SCD is often the first clinical presentation in patients with SQTS. However, arrhythmic risk stratification is presently unsatisfactory in asymptomatic patients. In this context, artificial intelligence-based electrocardiogram (ECG) analysis has never been applied to refine risk stratification in patients with SQTS. The purpose of this study was to analyze ECGs from SQTS patients with the aid of different AI algorithms to evaluate their ability to discriminate between subjects with and without documented life-threatening arrhythmic events.

The study group included 104 SQTS patients, 37 of whom had a documented major arrhythmic event at presentation and/or during follow-up. Thirteen ECG features were measured independently by three expert cardiologists; then, the dataset was randomly divided into three subsets (training, validation and testing). Five shallow neural networks were trained, validated and tested to predict subject specific class (non-event/event) using different subsets of ECG features. Additionally, several Deep Learning and Machine Learning algorithms, such as Vision Transformer, Swin Transformer, MobileNetV3, EfficientNetV2, ConvNextTiny, Capsule Networks and logistic regression were trained, validated and tested directly on the scanned ECG images, without any manual feature extraction. Furthermore, a shallow neural network, a 1-D Transformer classifier and a 1-D CNN were trained, validated and test on ECG signals extracted from the aforementioned scanned images. Classification metrics were evaluated by means of: sensitivity; specificity; positive and negative predictive values; accuracy; and area under the curve.

Results prove that Artificial Intelligence can help clinicians in better stratifying arrhythmic risk in patients with SQTS. In particular, shallow neural networks processing features showed the best performance in identifying patients that will not suffer from a potentially lethal event. This could pave the way to a refined ECG-based risk stratification in this group of patients, potentially helping in saving the lives of young and otherwise healthy individuals.

Keywords: Artificial Intelligence; Shallow Learning; Deep Learning; Short QT syndrome; Electrocardiogram; Sudden Cardiac Death; Risk Stratification; Vision Transformers.

Citation: To be added by editorial staff during production.

Academic Editor: Firstname Lastname

Received: date
Revised: date
Accepted: date
Published: date

1. Introduction

Short QT syndrome (SQTS) is an inherited channelopathy, which was first linked to an increased risk to develop atrial fibrillation [1] and, then, to sudden cardiac death (SCD) [2] in young and otherwise healthy individuals. In 2003, Gaita et al. [2] described two unrelated families with a corrected QT interval (QTc) less than 300 ms and familial history of SCD, outlining SQTS as a novel clinical entity with an autosomal dominant pattern of inheritance. Shortly after, the genetic nature of SQTS was confirmed by the discovery of gain-of-function mutations in potassium channels [3–5]. Subsequently, mutations in other channels were described [6,7], even though the yield of genetic screening in these patients remains low (less than 30 %).

According to 2022 European Society of Cardiology guidelines [8], SQTS diagnosis is recommended in case of a QTc ≤ 360 ms and one or more of the following: confirmed pathogenic mutation; family history of SQTS; survival from a ventricular fibrillation/tachycardia (VF/VT) episode in the absence of heart disease. Moreover, SQTS diagnosis should be considered in the presence of a QTc ≤ 320 ms or ranging between 320 and 360 ms together with history of arrhythmic syncope; finally, the diagnosis may be considered in case of QTc ranging between 320 and 360 ms and family history of SD below the age of 40 years.

Clinical presentation of SQTS patients is highly heterogeneous; in particular, the most frequent (up to 32 %) symptomatic presentation is SCD, which is often the first clinical manifestation of the disease [9]. As a consequence, it is extremely important to discriminate, within asymptomatic patients, those who will experience SCD from those who will not.

Until now, arrhythmic risk stratification in asymptomatic SQTS patients has been suboptimal, since no solid clinical or electrocardiographic parameters predicting life-threatening arrhythmic events are currently available [7, 9–12].

The use of artificial intelligence (AI) in medicine is relatively recent, if compared to other fields (such as speech analytics); however, it is rapidly receiving widespread interest due to high expectations in terms of improving healthcare and reducing related costs [13–17]. In particular, the application of AI in ECG analysis has recently gained tremendous momentum due to the fact that ECG constitutes an ideal substrate for AI application, being a low-cost and widely adopted cardiological tool [18]. Different groups reported favorable results obtained with AI-based ECG analysis in several clinical settings such as: prediction of underlying atrial fibrillation in patients presenting with sinus rhythm [19]; arterial blood pressure estimation [20–24]; estimation of age and sex [25]; prediction of underlying cardiac contractile dysfunction [26] and of hyperkalemia [27]; arrhythmia classification [28–30]; detection of hypertrophic cardiomyopathy [31]; early detection of cardiovascular autonomic neuropathy [32]; drug development [33]; and, more in general, heartbeat classification [34–36]. The high-level discrimination capabilities of such AI models, which showed very good predictive performances [37–39], together with the quickness, availability and cost-effectiveness of the ECG, highlight the high potential of AI-based ECG analysis. However, to our knowledge, despite its potential, AI-based ECG analysis has never been applied to SCD risk stratification in patients with SQTS.

The purpose of this study was to analyze ECGs from SQTS patients with the aid of different artificial intelligence systems in order to evaluate their ability to discriminate between subjects with and without documented arrhythmic events.

The rest of the paper is organized as follows: Sec. 2 describes the methodology; Sec. 3 presents the results, which are then discussed in Sec. 4; finally, Sec. 5 yields the conclusions.

2. Methods

2.1. Definitions and study population

The study group included a total of 104 subjects (see Table 1). To our knowledge, this is the first study to use AI for SQTS risk stratification; therefore, to avoid any bias, it was chosen to define SQTS in a very conservative way, as proposed by our group in 2011 [9], as the presence of a QT_c interval (Bazett's formula [40]) ≤ 340 ms; alternatively, SQTS was defined as a QT_c interval ≤ 360 ms (or a QT/QT_p ratio ≤ 88 %) [9, 41] associated with at least one of the following conditions: personal history of SCD, aborted sudden death (aSD) or syncope, familial history of SCD or SQTS. Eighty-four patients presented with relevant family history: 53 had familiarity for both SQTS and SCD, while the remaining showed familiarity only for SCD (n = 11) or SQTS (n = 20).

A major arrhythmic event was defined as the occurrence of SCD, aborted sudden death (aSD), and/or unexplained syncope. Overall, 37 patients developed a major arrhythmic event, both at presentation and/or during follow-up: 7 died suddenly (SCD), 19 had an aSD, while 11 had unexplained syncope. Conversely, 67 did not experience any major arrhythmic event.

To avoid event-related ECG alterations, the ECGs of patients with a major arrhythmic events were sampled far from the event (either before or after). In case of SCD, since it was not possible to acquire novel ECGs, it was used a baseline ECG recorded before the event occurred. In case of asymptomatic patients, it was selected a baseline ECG from the available ones.

Table 1. Study population characteristics.

Variables	N=104
Family history, No. (%)	84 (80.8)
SCD	11 (10.6)
SQTS	20 (19.2)
SCD and SQTS	53 (51.0)
Event occurrence, No. (%)	37 (35.6)
SCD	7 (0.7)
aSD	19 (18.3)
Unexplained Syncope	11 (10.6)

2.2. Dataset description and features

For each patient, data regarding both personal and family history were collected together with 12-lead ECG with a paper speed of either 25 mm/s or 50 mm/s, and a gain of 10 mm/mV.

ECG parameters (features) were measured with a 400% magnification (see Fig. 1) independently by three expert cardiologists from the lead with the highest T-wave amplitude (usually ranging from V2 to V5), including (see Fig. 1 right): RR interval; QT interval; QRS duration; J point – T peak ($J\text{-}T_p$); T peak – T end ($T_p\text{-}T_e$); J point – T end ($J\text{-}T_e$); and T-wave amplitude (T_{amp}). Furthermore, the following parameters were calculated: QT_p according to Rautaharju et al. formula [41], QT/QT_p, and the values of QT, J point – T peak, T peak – T end, and J point – T end corrected with Bazett's formula. QT interval was

measured according to the tangential method [40]. T peak was defined as the highest point of the T-wave. The complete feature set is summarized in Table 2.

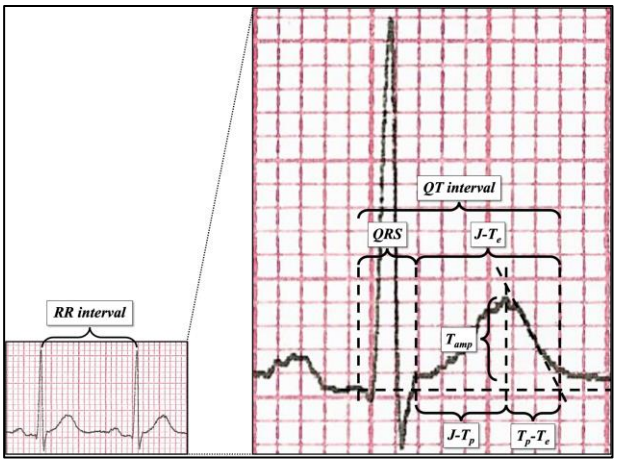

Figure 1. ECG parameter measurement after a 400% magnification.

Table 2. Input feature set description.

Feature	Description
RR (ms)	Interval between two R-waves
QT (ms)	Interval from the start of QRS complex and the end of T-wave (defined using tangential method); it expresses global duration of ventricular electrical activity, although used to evaluate ventricular repolarization
QT_c (ms)	QT interval corrected for heart rate using Bazett's formula $QT_c = QT/\sqrt{RR}$
QT_p (ms)	QT interval predicted with Rautaharju et al. formula $QT_p = 656/(1+HR/100)$
QRS (ms)	Interval between start and end of QRS complex; it expresses the duration of ventricular depolarization
J-T_p (ms)	Interval between J point (junction between the end of the QRS complex and the beginning of the ST segment) and the peak of the T-wave; it represents the early phase of repolarization
T_p-T_e (ms)	Interval between the peak of the T-wave and its end (defined using tangential method); it is a correlate of global dispersion of repolarization
J-T_e (ms)	Interval between J point (junction between the end of the QRS complex and the beginning of the ST segment) and the end of T-wave (defined using tangential method); it expresses the effective duration of ventricular repolarization
T_{amp} (mV)	Amplitude of T-wave measured from isoelectric line up to its peak
cJ-T_p (ms)	Interval between J point and the peak of the T-wave corrected with Bazett's formula
cT_p-T_e (ms)	Interval between the peak of the T-wave to its end corrected with Bazett's formula
cJ-T_e (ms)	Interval between J point and the end of T-wave corrected with Bazett's formula
QT/QT_p	Ratio among the QT interval and the QT_p

2.3. Neural networks

Neural networks are a set of algorithms, modeled on the human brain functions, designed to recognize patterns, i.e. the relationships, between the input and the output (target) signals [42]. In this work, two complementary approaches (human-engineered features vs automatic feature extraction), have been tested to perform SQTS risk stratification. In the former scenario, cardiologists have measured the features reported in Table 2 and, then, this set has been fed to a shallow learning model, while, in the latter case, ECG scans have been fed directly to the Vision Transformer, without any prior feature extraction phase. Human-engineered features have a direct, clear, medical explanation; for example, the R-R interval refers to the time between two heartbeats. However, the shallow neural network performance are highly affected by the input feature choice; since SQTS risk stratification is still an open problem, feature selection is not straightforward. On the other side, Deep Learning models are able to automatically extract the most significant features from the training input images and, therefore, cannot be biased by human-based feature selection; however, they act as a black-box, which means they cannot provide any medical explanation of a good risk stratification performance. It is worth to mention that, given the limited size of the input dataset, it is probable that shallow neural network would work better than Deep Learning models.

There are pros and cons in both scenarios; however, given the above, both approaches are complementary and worthy to be explored in an experimental setting.

2.3.1. Shallow neural networks: human-engineered features

In a standard multi-layer perceptron (MLP) configuration, the input layer is made of a set of units (neurons), one per each feature, which work as an entry point to the neural network. Indeed, this layer consists of passive nodes, which do not modify the input, but only transmit the information to each neuron of the subsequent layer (also known as fully connected). The hidden layer has an arbitrary amount of neurons, which depends on the complexity of the problem at hand. Each hidden node combines the information received from each unit of the input layer to achieve a complex representation of the phenomenon under investigation. At this purpose, a non-linear activation function is employed, such as the hyperbolic tangent sigmoid. Finally, the output layer yields the input data classification by means of the softmax function [43].

Due to the dataset size and the use of human-engineered features, it was chosen to use a shallow learning model. At this purpose, a feed-forward fully connected neural network with one hidden layer was designed. Different hidden layer sizes have been tested to evaluate the corresponding network classification performance; the best performing architecture has 30 and 1 neurons in the hidden and output layers, respectively, while the input layer size depends on the experiment (i.e. on the size of the input feature set). Aside from achieving superior performance, such configuration has a reduced capacity, due to the lower number of neurons in the hidden layer. This feature can help prevent overfitting, which is likely to occur when analyzing such small datasets, threatening to invalidate final results. Hidden units were equipped with hyperbolic tangent sigmoid transfer function, while the output layer used softmax to yield classification. The network training was performed using the scaled conjugate gradient (SCG) [44] technique to minimize the cross-entropy error function.

2.3.2. Shallow neural networks: signals

A basic multi-layer perceptron has also been fed with ECG signals extracted from the two-heartbeat image crops that will be detailed in the next sections. A signal extraction tool [45] was used, yielding 500-samples numerical signals for precordial leads (V1 to V3, since leads V4 to V6 were too noisy to be digitized on several images). This process was remarkably complicated and time-consuming. An example of extracted numerical ECG signal is shown in Figure 2.

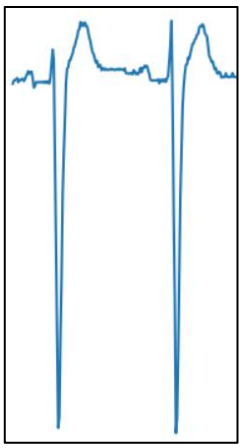

Figure 2. Example of a digitized ECG signal extracted from a scanned image

Several configurations for the neural network were tested; the best perfoming one had 50 neurons in the hidden layer and 1 neuron in the output layer. The same considerations for the feature approach apply for this case.

2.3.3. Deep Learning models: Convolutional Neural Networks

Despite being arguably surpassed by more recent models, Convolutional Neural Networks (CNNs) are still the most common Deep Learning models for computer vision applications. CNNs apply different *kernels* over the input image in order to extract relevant features [46]. Stacking several layers, each one with a different kernel in charge of capturing a specific aspect of the picture, eventually allows the network to collect enough information to execute tasks like classification, segmentation, object detection and the like.

CNN architectures deployed for this work are EfficientNetV2S, MobileNetV3 and ConvNextTiny [47][48][49], together with a 1-D CNN applied to numerical signals extracted from images. Apparently, this approach did not yield the expected results, as detailed in the next sections.

2.3.4. Deep Learning Models: Vision Transformer and Swin Transformer

A different type of approach is offered by the Vision Transformer (or ViT), a deep neural network designed as a "computer vision version" of the original Transformer [50, 51].

This architecture processes images by dividing them into equally-sized patches, which are subsequently embedded and fed to the transformer. The embedding process also accounts for patch position within the image, thus retaining the positional information of each patch. The resulting vector is then processed inside the Transformer encoder by blocks called heads, which exploit the attention mechanism [52] to evaluate the information associated to each patch, and how these "patches of information" are related to each other. Multiple heads perform these operations at once, allowing the network to gather knowledge about the global context of the picture. The encoder output is then fed to a multi-layer perceptron to classify the image on the basis of the information that the network was able to extract from it.

The stages of the Vision Transformer in image analysis are in many ways similar to what the human eye and brain do when looking at a picture, trying to grasp its meaning by merging information coming from details and knowledge gathered from the global picture, providing a tool that is capable to extract features autonomously. Conversely, shallow learning models require ECG features as inputs to the network, thus implying the necessity to gather medical knowledge about the topic before network deployment.

A different version of the Vision Transformer, called *Shifted Window Transformer* (Swin Transformer) was developed trying to make the basic ViT architecture better suited to vision tasks [53]. In fact, visual entities can undergo large variations, and image pixels can have a significant resolution when compared to word in text. In order to overcome these issues, the Swin Transformer's hierarchical architecture can adapt to different scales, and its computational complexity varies linearly with image size.

This model was applied to ECG images to assess performance against the Vision Transformer. Both Vision and Swin Transformers were pretrained on the ImageNet database [54] and fine-tuned on scanned ECG images. In addition, a 1-D version of the original Transformer encoder was applied to numerical signal extracted from images.

2.3.5. Deep Learning models: Capsule neural networks

Capsule neural networks (CapsNets) were designed to overcome some of CNNs main limitations, like lacking the capability to preserve spatial relationships among image elements [55]. In fact, to mention an "infamous" example, a CNN would typically identify a human face even when its elements – e.g. nose, mouth, eyes – are misplaced with respect to where they are expected to lie. With the introduction of *capsule modules* and *dynamic routing*, these neural models are able to capture the orientation of parts within an image.

2.3.6. Logistic Regression

One of the most common machine learning algorithms. Logistic Regression fits input data along a sigmoid function, assigning it to different classes according to where it lays along the function plot [56]. This classifier can be fed with images to perform classification, and in this case, it was applied on scanned ECG images.

2.4. Data pre-processing

The input dataset has been pre-processed to enhance network training and avoid overfitting.

In the case of the Shallow Learning Model, to reduce noise in data and avoid bias in the network training, data have been statistically normalized (*z-score*) to make the network able to intrinsically determine each input feature importance for classification. Indeed, without this step, it would have been possible that some features masked some others, preventing the network to understand the real contribution of each input attribute to SQTS risk stratification.

On the other side, for Deep Learning Models, images were initially cropped to remove all the elements in the bordering part that do not strictly belong to an ECG chart. Said elements are usually accompanying information (e.g.; annotations) which are considered to carry no relevant data for the given task. Yet, if not removed, their information content could erroneously be marked as noteworthy by the model, thus introducing unwanted biases in classification. Figure 3 shows an example of ECG image before and after the initial cropping.

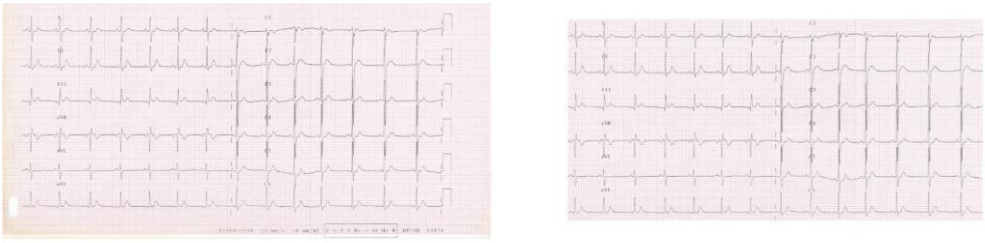

(**a**) (**b**)

Figure 3. (**a**) ECG image before cropping; (**b**) ECG image after cropping.

In order to try and isolate possible elements of the image carrying more information, images were later cropped to contain only two heartbeats, leading to two additional versions of the dataset: one containing two-heartbeat-crops for each precordial lead (e.g.: V1 only, V2 only and so on, see Figure 4), and another one containing all two-heartbeat-crops for all precordial leads (which are considered to hold more information than peripheral leads with respect to SQTS diagnosis).

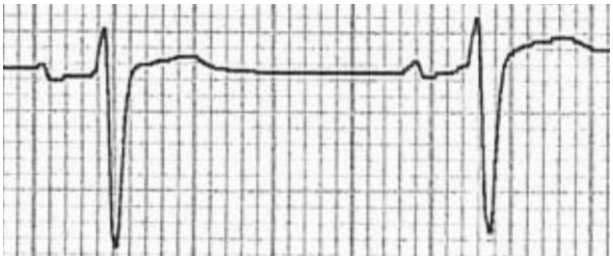

Figure 4. Two-heartbeat crop on a single precordial lead from a scanned image

Subsequently, data augmentation techniques were implemented for all Deep Learning models in order to help the network achieve better results during training. In particular, input images went through the following stages undergoing the RandAugment method for image augmentation [57]: cropping at center; normalizing; horizontal flipping with a 50% probability of rotation occurring; random cropping and resizing; final resizing to the initial size. This process was especially necessary to try to level out the strong data

imbalance in between the two classes, which would otherwise lead to a penalization of the model's generalization capabilities.

Another approach was the extraction of numerical signals from the two-heartbeat crops on leads V1, V2 and V3, with the purpose of trying and retrieving the information retained in the original ECG signals that were acquired by the time data was collected. This was done by exploiting the specific tool mentioned previously in Section 2.3.2.

For all AI models, both the input and target sets were randomly divided into three sets as follows: 70 % for training; 10 % to validate that the network is generalizing and to stop training before overfitting; and the remaining 20 % to independently test the network classification performance. To ensure the input data distribution (i.e. the amount of non-event/event cases) was preserved in the three sets, the random division has been performed separately for non-event and event subsets.

2.5. Classification metrics

Classification accuracy was estimated analyzing the confusion matrices and the associated ROC curve. The former, shown in Fig. 5, measures the amount of times the network correctly classify the input; in this sense, it yields an estimate of how much a single class (negative/positive), i.e. a medical condition (non-event/event), was understood by the neural model. The rows and the columns correspond to the actual (aka target) and predicted classes, respectively. The diagonal cells correspond to the true observations (True Positive and True Negative), correctly classified, while the off-diagonal cells correspond to the false observations (False Positive and False Negative), incorrectly classified.

To better analyze the network performance, five advanced classification metrics can be derived from the confusion matrix:

- *Sensitivity*, also referred as *True Positive Rate* or *Recall*: it measures the percentage of positive examples correctly labelled as positive by the classifier. In medicine, highly sensitive tests are generally used for screening purposes, due to their ability to rule out the disease/event occurrence.

- *Specificity*, also known as *True Negative Rate*: it measures the percentage of negative examples correctly labelled as negative by classifier. In medicine, highly specific tests are typically used for confirmation purposes, due to their ability to rule in the disease/event occurrence.

- *Positive predictive value (PPV)*, also known as *Precision*: the ratio between the total number of correctly classified positive examples and the total number of predicted positive examples. It yields the correctness achieved in positive prediction, which means it measures the likelihood that an event will truly occur given a corresponding network positive outcome.

- *Negative predictive value (NPV)*: the ratio between the total number of correctly classified negative examples and the total number of predicted negative examples. It yields the correctness achieved in negative prediction, which means it measures the likelihood that an event will truly not occur given a corresponding network negative outcome.

- *Accuracy*: the percentage of correct predictions. It is an average measure of the network quality.

- *F1-Score*: it is the harmonic mean of PPV and Sensitivity. It is better suited for unbalanced datasets than accuracy.

		Predicted: Negative	Predicted: Positive	
Actual	Negative	True Negative (**TN**)	False Positive (**FP**)	**Specificity** $\frac{TN}{TN+FP}$
	Positive	False Negative (**FN**)	True Positive (**TP**)	**Sensitivity** $\frac{TP}{TP+FN}$
		NPV $\frac{TN}{TN+FN}$	**PPV** $\frac{TP}{TP+FP}$	**Accuracy** $\frac{TP+TN}{TP+FP+TN+FN}$

Figure 5. Confusion matrix example: rows yield the real (actual) labels, columns the predicted ones, i.e. the network outputs

Despite accuracy provides a single global measure of the classification quality, it is just a mean value of the network performances. On the contrary, the area under the ROC curve (AUC) yields a more precise measure (the higher the best) of the predictive accuracy because it represents the probability that a randomly chosen positive sample is ranked higher than a corresponding negative one.

3. Results

The classification ability of the proposed shallow learning model has been tested on different input configurations, i.e. different input human-engineered feature sets, to study which features were the most relevant to correctly discriminate among subjects who will have an event from those who will not. In this sense, it was investigated the importance of the QT interval and of the T wave in distinguishing the two classes (i.e. non-event/event). Therefore, the experiments could be grouped into five categories as per Table 3:

- QT : only the QT related features were considered;
- T_{wave} : only the T wave features were considered;
- QT + T_{wave} : both the QT related and T wave features were considered;
- $T_{wave\ ext}$: T wave features were considered together with their Bazzett-corrected values;
- All : all input features were considered.

Table 3. Input dataset taxonomy.

	Input configurations				
Feature	**QT**	**T_{wave}**	**QT+T_{wave}**	**$T_{wave\ ext}$**	**All**
RR (ms)	✓		✓	✓	✓
QT (ms)	✓		✓		✓
QT_c (ms)	✓		✓		✓

QT_p (ms)	✓		✓		✓
T_{amp} (mV)	✓	✓	✓	✓	✓
QRS (ms)	✓		✓		✓
J-T_p (ms)		✓	✓	✓	✓
T_p-T_e (ms)		✓	✓	✓	✓
J-T_e (ms)		✓	✓	✓	✓
cJ-T_p (ms)				✓	✓
cT_p-T_e (ms)				✓	✓
cJ-T_e (ms)				✓	✓
QT/QT_p					✓

To assess the network classification performances, sensitivity, specificity, PPV, NPV, and accuracy were evaluated. The results on the test set (see Table 4), which checks the ability of the models to perform on new and previously unseen samples, can be summarized as follows:

- Sensitivity: it is generally low in all configurations with a maximum value of 63.6 % in the T_{wave} input configuration and a minimum of 36.4 % in the All configuration.
- Specificity: this metric is generally high across all the different explored input configurations, with values ranging from 85 % (T_{wave}) to 95 % (QT, $T_{wave\ ext}$ and All).
- PPV and NPV: these two metrics do not show optimal values in any of the proposed input configurations; in particular, PPV showed better results as compared to NPV (maximum PPV: 83.3 % in QT and $T_{wave\ ext}$; maximum NPV: 81 % in T_{wave}).
- Accuracy: this evaluation metric is generally suboptimal across all the evaluated configurations, with all the configurations showing 77.4 % accuracy, with the only exception of the All input configuration, which showed a slightly reduced accuracy in the test set (74.2 %).
- F1-Score: this evaluation metric is generally suboptimal across all the evaluated configurations, with the T_{wave} one reaching the highest value of 66.6, and QT+T_{wave} showing roughly the same performance (63.1).

Table 4. Shallow network (human-engineered features) classification performances: Sensitivity, Specificity, PPV, NPV, Accuracy, F1-Score. Values are in percentage. The highest values per each metric are highlighted in bold.

	QT	T_{wave}	QT+T_{wave}	$T_{wave\ ext}$	All
Sensitivity	45.5	**63.6**	54.5	45.5	36.4
Specificity	**95.0**	85.0	90.0	**95.0**	**95.0**
PPV	**83.3**	70.0	75.0	**83.3**	80.0
NPV	76.0	**81.0**	78.3	76.0	73.1
Accuracy	**77.4**	**77.4**	**77.4**	**77.4**	74.2
F1-Score	58.9	**66.6**	63.1	58.9	50.0

Finally, Table 5 reports the AUC values for the five evaluated feature sets. While training set AUCs are generally satisfying, the same cannot be said for test set AUCs: in fact, as can be appreciated, AUC values drop to poor values (AUC < 0.60) or just acceptable values (AUC 0.60-0.70) in all the configurations, except for QT + T_{wave} configuration, which present a good AUC also in the testing set (0.81).

Table 5. Shallow network (human-engineered features) classification performances: AUC.

	QT		T_{wave}		QT+T_{wave}		$T_{wave\ ext}$		All	
	Training	**Test**	**Training**	**Test**	**Training**	**Test**	**Training**	**Test**	**Training**	**Test**
AUC	0.86	0.58	0.75	0.67	0.85	0.81	0.72	0.59	0.76	0.53

Tables 6 and 7 summarize the results for the other approaches (signal and image analysis). Reported metrics are the test accuracy and the AUC scores obtained by feeding the networks with signals and single lead images. Results are quite similar, regardless the input type and/or the network architecture: apparently, none of those methods is able to capture any significant difference between the two categories, interpreting every input as a case without SCD event.

Table 6. Signal classification approach performances: Test Accuracy (percentage) and AUC.

	Shallow network	**1-D CNN**	**1-D Transformer**
Test Accuracy	63.6	64.0	64.0
AUC	0.50	0.51	0.51

Table 7. Image classification approach performances: Test Accuracy (percentage) and AUC.

	Efficient-NetV2S	**MobileNetV3**	**ConvNextTiny**	**Vision Transformer (ViT)**	**Swin Transformer**	**Capsule Networks**	**Logistic Regression**
Test Accuracy	56.2	56.2	65.6	63.3	64.1	65.0	55.0
AUC	0.47	0.47	0.55	0.52	0.50	0.51	0.45

3.1. Comparison with classical machine learning algorithms

Since the dataset is very small (104 samples and at most 13 features), 1-hidden-layer perceptron is not guaranteed to perform better than other classical ML models. Therefore, to better assess the quality of the proposed shallow learning model, it was performed an additional comparison with classical machine learning algorithms like: logistic regression [61], decision tree [62], boosted decision tree [62], bagged decision tree [63], support vector machine (SVM) [62], K-nearest neighbors (KNN) [64]. Also, PCA feature selection technique [65] was employed as preprocessing, retaining 90% of the overall explained variance, to see if reducing the input space would imply a improvement in the classification [66].

Table 8 yields the results on the test set, where different setting of these methods were reported. More in detail:

- Fine Tree, Medium Tree, Coarse Tree: decision tree with Gini's diversity index as split criterion and a maximum number of splits equal to 100, 20, 4, for Fine, Medium, Coase, tree, respectively.

- Boosted decision tree: ensemble of decision trees using AdaBoost algorithm (maximum number of splits: 20, number of learners: 30, learning rate: 0.1).
- Bagged decision tree: ensemble of decision trees [62] using Bag algorithm (maximum number of splits: 72, number of learners: 30).
- SVM: support vector machines [62], with different kernel functions: linear; quadratic; cubic; Gaussian with kernel scale equal to 0.5 (Fine Gaussian), 2 (Medium Gaussian), and 8 (Coarse Gaussian).
- Fine KNN, Medium KNN, Coarse KNN: k-nearest neighbor algorithm using Euclidean distance as metric and a number of neighbors equal to 1, 10, 100, for Fine, Medium, Coase, KNN, respectively.
- Cosine KNN: k-nearest neighbor algorithm using a number of neighbors equal to 10 and cosine distance as metric.
- Cubic KNN: k-nearest neighbor algorithm using a number of neighbors equal to 10 and Minkowsky distance as metric.

Despite some of these methods show promising results (i.e. 71.0 % of accuracy), no one reaches the same accuracy of the Shallow Learning (i.e. 77.4 %). Only Coarse Tree with PCA arrives to 74.2 % of accuracy, still below Shallow Learning one. PCA behavior is not conclusive, since in some cases it improves performances, while in some other cases it worsen them, even in the same technique; as an example, see Medium Tree vs Coarse Tree, or Quadratic SVM vs Cubic SVM.

Table 8. Accuracy classification performances of state-of-the-art ML methods on the five input configuration, with or without PCA data preprocessing (90 % of explained variance retained). Values are in percentage. The highest values per each column are highlighted in bold.

	QT		**T_{wave}**		**QT+T_{wave}**		**$T_{wave\ ext}$**		**All**	
	No PCA	**PCA**	**No PCA**	**PCA**	**No PCA**	**PCA**	**No PCA**	**PCA**	**No PCA**	**PCA**
Logistic Regression	58.1	64.5	64.5	**67.7**	58.1	64.5	58.1	**64.5**	61.3	64.5
Fine Tree	67.7	58.1	48.4	54.8	51.6	**71.0**	54.8	**64.5**	48.4	64.5
Medium Tree	67.7	58.1	48.4	54.8	51.6	**71.0**	54.8	**64.5**	48.4	64.5
Coarse Tree	58.1	**74.2**	58.1	58.1	58.1	67.7	45.2	**64.5**	45.2	58.1
Boosted Trees	54.8	67.7	54.8	64.5	64.5	**71.0**	64.5	45.2	41.9	54.8
Bagged Trees	64.5	67.7	54.8	45.2	**67.7**	64.5	58.1	58.1	58.1	67.7
Linear SVM	64.5	64.5	64.5	64.5	64.5	64.5	64.5	**64.5**	64.5	64.5
Quadratic SVM	**71.0**	58.1	**67.7**	64.5	64.5	**71.0**	54.9	61.3	64.5	**71.0**
Cubic SVM	58.1	64.5	54.8	54.8	58.1	67.7	41.9	58.1	54.8	67.7
Fine Gaussian SVM	64.5	71.0	58.1	58.1	64.5	64.5	61.3	**64.5**	64.5	61.3
Medium Gaussian SVM	64.5	64.5	61.3	61.3	64.5	64.5	64.5	**64.5**	**67.7**	64.5
Coarse Gaussian SVM	64.5	64.5	64.5	64.5	64.5	64.5	64.5	**64.5**	64.5	64.5
Fine KNN	64.5	67.7	64.5	58.1	51.6	58.1	61.3	54.9	51.6	61.3
Medium KNN	54.8	64.5	61.3	61.3	61.3	54.8	**67.7**	58.1	**67.7**	54.8
Coarse KNN	64.5	64.5	64.2	64.5	64.5	64.5	64.5	**64.5**	64.5	64.5
Cosine KNN	54.8	64.5	61.3	61.3	64.5	58.1	**67.7**	58.1	64.5	61.3
Cubic KNN	58.1	64.5	61.3	61.3	61.3	58.1	**67.7**	58.1	**67.7**	58.1

4. Discussion

SQTS is an inherited channelopathy related to increased risk of SCD. SCD is often the first symptomatic presentation, demanding an important effort to better stratify the arrhythmic risk in patients who are still asymptomatic at medical evaluation. Until now, risk stratification in asymptomatic patients has been unsatisfactory. To our knowledge, this is the first work using an AI-based approach to analyze ECG in patients with SQTS, in order to refine arrhythmic risk stratification. In this study, we used two different AI-based approaches to this purpose: the first approach requires manual features extraction from the ECG, which are used as inputs for shallow learning models; other approaches directly use the scanned ECG image or the signal extracted from it as input, automatically performing feature extraction. The main findings are summarized in the following.

Shallow learning models based on different configuration of manually extracted (human-engineered) ECG features achieved suboptimal performance, in particular regarding the NPV, which never overcomes 81 %; this is clinically relevant, since it means 2 out of 10 patients with an event are incorrectly classified in the non-event group, potentially leading to under-treatment.

All other approaches do not seem to grasp any significant difference between the two classes, and end up considering each input as a case with no SCD event. There are several possible factors that might have influenced such results:

- Scanned ECG images were extremely different from each other, in terms of resolution, format, color, background grid color, and most of them suffered a noisy, poor quality; this hindered the possibility to develop a consistent preprocessing procedure that could work efficiently on all dataset images.

- Dataset cardinality is particularly low; this could represent an obstacle for some of the Deep Learning models chosen, both for the image and the signal approach. In fact, such architectures often contain a vast number of parameters, and are usually trained on very large datasets.

- Image cropping was performed manually, both for lead isolation and signal digitization; this might introduce some errors due to the lack of specific methods and criteria for accurate and precise cropping area definition.

- The image and signal approaches were conceived to be specular to the feature approach: tested models were supposed to automatically extract relevant features in an unbiased manner, potentially uncovering aspects of the ECG chart that can enrich the knowledge about SQTS, and unveil elements that can hint to an increased risk of SCD event. Therefore, this methodology cannot leverage any a priori information that could steer feature search towards a specific direction.

These results suggest that AI-based ECG analysis, in particular using the features approach, might help in refining risk stratification in SQTS patients, supporting clinical decision-making in a context where incorrect risk appraisal might translate in the death of young and otherwise healthy individuals. A refined risk stratification means that the clinician may offer the patients the most appropriate treatment to prevent SCD, including cardiac devices. Implantable Cardioverter-Defibrillator (ICD) still represents the mainstay of treatment for patients with SQTS who are survivors of SCD or have documented spontaneous sustained VT [58], despite significant risk of device-related complications, such as inappropriate shocks (33%), device-related infection (10%), lead failure and fracture

(21%) and psychological distress (3.5%) [59,60]. In this sense, a better risk stratification might not just lead to earlier adoption of life-saving therapy to patients deemed at higher risk of SCD, but also to also to avoiding implantation of ICD in low-risk patients, potentially sparing the risk of device-related complications.

4.1. Study limits

The present work has some limitations, which need to be addressed. First, we acknowledge that the number of patients was limited; however, it should be borne in mind that SQTS is a rare disease, and this constitutes the widest cohort of SQTS patients published so far. Given the limited amount of ECGSs, it was not possible to refine the analysis to different subgroups, since the results would have been not significant from a statistical point of view.

For the shallow learning model, ECG features were not automatically extracted, but manually calculated by three experienced cardiologists (albeit with a 400 % magnification to minimize measurement errors), which is prone to errors in manual measurement. Moreover, it suffers from an implicit bias over the selected features set: although the thirteen features were selected based on the current medical knowledge, they could not be the more relevant ones to perform SQTS risk stratification. Further studies with different features sets should be considered. Future works will investigate different ways of feature selection, e.g. L1 regularization, and deepen the relationship among the features and the classification performances.

Finally, to increase generalizability, the results presented in this study will be verified on an external SQTS population coming from different regions or medical centers, to better assess their reliability.

5. Conclusions

Short QT syndrome is an inherited channelopathy linked with an increased risk of SCD in young and otherwise healthy individuals. Clinical presentation of patients affected by SQTS is highly heterogeneous, with SCD often being the first clinical presentation, and risk stratification is particularly challenging in asymptomatic subjects.

The analysis of ECG from SQTS patients with the aid of neural networks shows promising results in terms of discriminating between subjects with and without documented arrhythmic events. This could pave the way to a refined ECG-based risk stratification in this group of patients, potentially helping in saving the lives of young and otherwise healthy individuals, such as the initial study performed on the Brugada syndrome [62].

Future studies should focus on automatic calculation of the features from digital ECG recordings (either using raw digital ECG data or digitized data from paper-based ECG). This will guarantee an increased reproducibility if compared to manual extraction of relevant ECG features. In addition, other Deep Learning models, assessing the whole raw digital ECG signal and/or ECG images, should also be explored and should be compared to other architectures. As an example, images will be converted to the frequency domain to apply frequency-domain filters or Wiener filters for noise reduction, so that it will be

possible to provide cleaner input to vision-based Deep Learning models. In parallel, authors will continue to collect SQTS ECGs of subjects which have developed an event to increase the cardinality of the dataset and further validate the proposed approach; at this purpose, it will be probably needed to include different cohorts coming from different regions and medical centers. Finally, data augmentation by means of GANs, will be explored to increase the amount of ECG images and, thus, the classification performance.

Author Contributions: Conceptualization, F.G., E.P., and V.R.; methodology, V.R., E.P., and S.C.; software, V.R. and S.C.; validation, V.R., E.P. and S.C.; formal analysis, Pi.M., V.R., Ph.M., and S.C.; investigation, F.G., C.G., and Pi.M.; resources, E.P., F.G. and C.G.; data curation, Pi.M., Ph.M., and C.G.; writing—original draft preparation, V.R., S.C., Pi.M and C.G.; writing—review and editing, C.G., V.R., Ph.M., and F.G.; visualization, S.C. and V.R.; supervision, F.G., E.P., and C.G.; project administration, E.P., and V.R.; funding acquisition, E.P., V.R., and C.G. All authors have read and agreed to the published version of the manuscript.

Funding: This research has been partly funded by the BrS-AI-ECG project of the Italian Ministry of Foreign Affairs and International Cooperation. Dr. Randazzo also acknowledges funding from the research contract no. 32-G-13427-2 (DM 1062/2021) funded within the Programma Operativo Nazionale (PON) Ricerca e Innovazione of the Italian Ministry of University and Research.

Institutional Review Board Statement: The study was conducted according to the guidelines of the Declaration of Helsinki, and approved by the Institutional Review Board of Città della Salute e della Scienza Hospital, Turin, Italy (Protocol code: 248/2017, date of approval: February 22th, 2017).

Informed Consent Statement: Informed consent was obtained from all subjects involved in the study.

Data Availability Statement: The data presented in this study are available on request from the corresponding author.

Acknowledgments: Authors thank Annunziata Paviglianiti and Andrea Saglietto for the initial support.

Conflicts of Interest: The authors declare no conflict of interest.

References

1. Gussak, I.; Brugada, P.; Brugada, J.; Wright, R.S.; Kopecky, S.L.; Chaitman, B.R.; Bjerregaard, P. Idiopathic Short QT Interval:A New Clinical Syndrome?. Cardiology 2000, 94, 99–102, doi:10.1159/000047299.

2. Gaita, F.; Giustetto, C.; Bianchi, F.; Wolpert, C.; Schimpf, R.; Riccardi, R.; Grossi, S.; Richiardi, E.; Borggrefe, M. Short QT Syndrome: A Familial Cause of Sudden Death. Circulation 2003, 108, 965–970, doi:10.1161/01.CIR.0000085071.28695.C4.

3. Brugada, R.; Hong, K.; Dumaine, R.; Cordeiro, J.; Gaita, F.; Borggrefe, M.; Menendez, T.M.; Brugada, J.; Pollevick, G.D.; Wolpert, C.; et al. Sudden Death Associated With Short-QT Syndrome Linked to Mutations in HERG. Circulation 2004, 109, 30–35, doi:10.1161/01.CIR.0000109482.92774.3A.

4. Bellocq, C.; van Ginneken, A.C.G.; Bezzina, C.R.; Alders, M.; Escande, D.; Mannens, M.M.A.M.; Baró, I.; Wilde, A.A.M. Mutation in the KCNQ1 Gene Leading to the Short QT-Interval Syndrome. Circulation 2004, 109, 2394–2397, doi:10.1161/01.CIR.0000130409.72142.FE.

5. Priori, S.G.; Pandit, S.V.; Rivolta, I.; Berenfeld, O.; Ronchetti, E.; Dhamoon, A.; Napolitano, C.; Anumonwo, J.; di Barletta, M.R.; Gudapakkam, S.; et al. A Novel Form of Short QT Syndrome (SQT3) Is Caused by a Mutation in the KCNJ2 Gene. Circulation Research 2005, 96, 800–807, doi:10.1161/01.RES.0000162101.76263.8c.

6. Walsh, R.; Adler, A.; Amin, A.S.; Abiusi, E.; Care, M.; Bikker, H.; Amenta, S.; Feilotter, H.; Nannenberg, E.A.; Mazzarotto, F.; et al. Evaluation of Gene Validity for CPVT and Short QT Syndrome in Sudden Arrhythmic Death. European Heart Journal 2022, 43, 1500-1510, doi: 10.1093/eurheartj/ehab687.

7. Mazzanti, A.; Kanthan, A.; Monteforte, N.; Memmi, M.; Bloise, R.; Novelli, V.; Miceli, C.; O, 'Rourke Sean; Borio, G.; Zienciuk, -Krajka Agnieszka; et al. Novel Insight Into the Natural History of Short QT Syndrome. Journal of the American College of Cardiology 2014, 63, 1300–1308, doi:10.1016/j.jacc.2013.09.078.

8. Zeppenfeld, K.; Tfelt-Hansen, J.; de Riva, M.; Winkel, B.G.; Behr, E.R.; Blom, N.A.; Charron, P.; Corrado, D.; Dagres, N.; de Chillou, C.; et al. 2022 ESC Guidelines for the Management of Patients with Ventricular Arrhythmias and the Prevention of Sudden Cardiac Death. Eur Heart J 2022, 43, 3997–4126, doi:10.1093/eurheartj/ehac262.

9. Giustetto, C.; Schimpf, R.; Mazzanti, A.; Scrocco, C.; Maury, P.; Anttonen, O.; Probst, V.; Blanc, J.-J.; Sbragia, P.; Dalmasso, P.; et al. Long-Term Follow-Up of Patients With Short QT Syndrome. Journal of the American College of Cardiology 2011, 58, 587–595, doi:10.1016/j.jacc.2011.03.038.

10. Rudic, B.; Schimpf, R.; Borggrefe, M. Short QT Syndrome – Review of Diagnosis and Treatment. Arrhythm Electrophysiol Rev 2014, 3, 76–79, doi:10.15420/aer.2014.3.2.76.

11. Anttonen, O.; Junttila, M.J.; Maury, P.; Schimpf, R.; Wolpert, C.; Borggrefe, M.; Giustetto, C.; Gaita, F.; Sacher, F.; Haïssaguerre, M.; et al. Differences in Twelve-Lead Electrocardiogram between Symptomatic and Asymptomatic Subjects with Short QT Interval. Heart Rhythm 2009, 6, 267–271, doi:10.1016/j.hrthm.2008.10.033.

12. Tülümen, E.; Giustetto, C.; Wolpert, C.; Maury, P.; Anttonen, O.; Probst, V.; Blanc, J.-J.; Sbragia, P.; Scrocco, C.; Rudic, B.; et al. PQ Segment Depression in Patients with Short QT Syndrome: A Novel Marker for Diagnosing Short QT Syndrome? Heart Rhythm 2014, 11, 1024–1030, doi:10.1016/j.hrthm.2014.02.024.

13. Topol, E.J. High-Performance Medicine: The Convergence of Human and Artificial Intelligence. Nature Medicine 2019, 25, 44–56, doi:10.1038/s41591-018-0300-7.

14. Valente, F.; Henriques, J.; Paredes, S.; Rocha, T.; de Carvalho, P.; Morais, J. A New Approach for Interpretability and Reliability in Clinical Risk Prediction: Acute Coronary Syndrome Scenario. Artificial Intelligence in Medicine 2021, 117, 102113, doi:10.1016/j.artmed.2021.102113.

15. Alfieri, F.; Ancona, A.; Tripepi, G.; Crosetto, D.; Randazzo, V.; Paviglianiti, A.; Pasero, E.; Vecchi, L.; Cauda, V.; Fagugli, R.M. A Deep-Learning Model to Continuously Predict Severe Acute Kidney Injury Based on Urine Output Changes in Critically Ill Patients. Journal of Nephrology 2021, doi:10.1007/s40620-021-01046-6.

16. Roberti, I., Lovino, M., Di Cataldo, S., Ficarra, E., & Urgese, G. Exploiting Gene Expression Profiles For The Automated Prediction Of Connectivity Between Brain Regions. International Journal Of Molecular Sciences 2019, 20, doi: 10.3390/ijms20082035.

17. de Siqueira, V.S.; Borges, M.M.; Furtado, R.G.; Dourado, C.N.; da Costa, R.M. Artificial Intelligence Applied to Support Medical Decisions for the Automatic Analysis of Echocardiogram Images: A Systematic Review. Artificial Intelligence in Medicine 2021, 120, 102165, doi:10.1016/j.artmed.2021.102165.

18. Siontis, K.C.; Noseworthy, P.A.; Attia, Z.I.; Friedman, P.A. Artificial Intelligence-Enhanced Electrocardiography in Cardiovascular Disease Management. Nature Reviews Cardiology 2021, 18, 465–478, doi:10.1038/s41569-020-00503-2.

19. Attia, Z.I.; Noseworthy, P.A.; Lopez-Jimenez, F.; Asirvatham, S.J.; Deshmukh, A.J.; Gersh, B.J.; Carter, R.E.; Yao, X.; Rabinstein, A.A.; Erickson, B.J.; et al. An Artificial Intelligence-Enabled ECG Algorithm for the Identification of Patients with Atrial Fibrillation during Sinus Rhythm: A Retrospective Analysis of Outcome Prediction. The Lancet 2019, 394, 861–867, doi:10.1016/S0140-6736(19)31721-0.

20. Baker, S.; Xiang, W.; Atkinson, I. A Hybrid Neural Network for Continuous and Non-Invasive Estimation of Blood Pressure from Raw Electrocardiogram and Photoplethysmogram Waveforms. Computer Methods and Programs in Biomedicine 2021, 207, 106191, doi:10.1016/j.cmpb.2021.106191.

21. Paviglianiti, A.; Randazzo, V.; Villata, S.; Cirrincione, G.; Pasero, E. A Comparison of Deep Learning Techniques for Arterial Blood Pressure Prediction. Cognitive Computation 2021, doi:10.1007/s12559-021-09910-0.

22. Paviglianiti, A.; Randazzo, V.; Cirrincione, G.; Pasero, E. Double Channel Neural Non Invasive Blood Pressure Prediction. In Proceedings of the Intelligent Computing Theories and Application; Huang, D.-S., Bevilacqua, V., Hussain, A., Eds.; Springer International Publishing: Cham, 2020; pp. 160–171.

23. Paviglianiti, A.; Randazzo, V.; Cirrincione, G.; Pasero, E. Neural Recurrent Approches to Noninvasive Blood Pressure Estimation. In Proceedings of the 2020 International Joint Conference on Neural Networks (IJCNN); July 2020; pp. 1–7.

24. Paviglianiti, A.; Randazzo, V.; Pasero, E.; Vallan, A. Noninvasive Arterial Blood Pressure Estimation Using ABPNet and VITAL-ECG. In Proceedings of the 2020 IEEE International Instrumentation and Measurement Technology Conference (I2MTC); May 2020; pp. 1–5.

25. Attia, Z.I.; Friedman, P.A.; Noseworthy, P.A.; Lopez-Jimenez, F.; Ladewig, D.J.; Satam, G.; Pellikka, P.A.; Munger, T.M.; Asirvatham, S.J.; Scott, C.G.; et al. Age and Sex Estimation Using Artificial Intelligence From Standard 12-Lead ECGs. Circulation: Arrhythmia and Electrophysiology 2019, 12, e007284, doi:10.1161/CIRCEP.119.007284.

26. Attia, Z.I.; Kapa, S.; Lopez-Jimenez, F.; McKie, P.M.; Ladewig, D.J.; Satam, G.; Pellikka, P.A.; Enriquez-Sarano, M.; Noseworthy, P.A.; Munger, T.M.; et al. Screening for Cardiac Contractile Dysfunction Using an Artificial Intelligence–Enabled Electrocardiogram. Nature Medicine 2019, 25, 70–74, doi:10.1038/s41591-018-0240-2.

27. Galloway, C.D.; Valys, A.V.; Shreibati, J.B.; Treiman, D.L.; Petterson, F.L.; Gundotra, V.P.; Albert, D.E.; Attia, Z.I.; Carter, R.E.; Asirvatham, S.J.; et al. Development and Validation of a Deep-Learning Model to Screen for Hyperkalemia From the Electrocardiogram. JAMA Cardiology 2019, 4, 428–436, doi:10.1001/jamacardio.2019.0640.

28. Wang, J.; Qiao, X.; Liu, C.; Wang, X.; Liu, Y.; Yao, L.; Zhang, H. Automated ECG Classification Using a Non-Local Convolutional Block Attention Module. Computer Methods and Programs in Biomedicine 2021, 203, 106006, doi:10.1016/j.cmpb.2021.106006.

29. Asl, B.M.; Setarehdan, S.K.; Mohebbi, M. Support Vector Machine-Based Arrhythmia Classification Using Reduced Features of Heart Rate Variability Signal. Artificial Intelligence in Medicine 2008, 44, 51–64, doi:10.1016/j.artmed.2008.04.007.

30. Ferretti, J.; Randazzo, V.; Cirrincione, G.; Pasero, E. 1-D Convolutional Neural Network for ECG Arrhythmia Classification. In Progresses in Artificial Intelligence and Neural Systems; Esposito, A., Faundez-Zanuy, M., Morabito, F.C., Pasero, E., Eds.; Smart Innovation, Systems and Technologies; Springer: Singapore, 2021; pp. 269–279 ISBN 9789811550935.

31. Rahman, Q.A.; Tereshchenko, L.G.; Kongkatong, M.; Abraham, T.; Abraham, M.R.; Shatkay, H. Utilizing ECG-Based Heartbeat Classification for Hypertrophic Cardiomyopathy Identification. IEEE Transactions on NanoBioscience 2015, 14, 505–512, doi:10.1109/TNB.2015.2426213.

32. Hassan, M.R.; Huda, S.; Hassan, M.M.; Abawajy, J.; Alsanad, A.; Fortino, G. Early Detection of Cardiovascular Autonomic Neuropathy: A Multi-Class Classification Model Based on Feature Selection and Deep Learning Feature Fusion. Information Fusion 2022, 77, 70–80, doi:10.1016/j.inffus.2021.07.010.

33. Sahli Costabal, F.; Matsuno, K.; Yao, J.; Perdikaris, P.; Kuhl, E. Machine Learning in Drug Development: Characterizing the Effect of 30 Drugs on the QT Interval Using Gaussian Process Regression, Sensitivity Analysis, and Uncertainty Quantification. Computer Methods in Applied Mechanics and Engineering 2019, 348, 313–333, doi:10.1016/j.cma.2019.01.033.

34. Dai, H.; Hwang, H.-G.; Tseng, V.S. Convolutional Neural Network Based Automatic Screening Tool for Cardiovascular Diseases Using Different Intervals of ECG Signals. Computer Methods and Programs in Biomedicine 2021, 203, 106035, doi:10.1016/j.cmpb.2021.106035.

35. Liu, H.; Zhao, Z.; Chen, X.; Yu, R.; She, Q. Using the VQ-VAE to Improve the Recognition of Abnormalities in Short-Duration 12-Lead Electrocardiogram Records. Computer Methods and Programs in Biomedicine 2020, 196, 105639, doi:10.1016/j.cmpb.2020.105639.

36. Monedero, I. A Novel ECG Diagnostic System for the Detection of 13 Different Diseases. Engineering Applications of Artificial Intelligence 2022, 107, 104536, doi:10.1016/j.engappai.2021.104536.

37. Green, M.; Björk, J.; Forberg, J.; Ekelund, U.; Edenbrandt, L.; Ohlsson, M. Comparison between Neural Networks and Multiple Logistic Regression to Predict Acute Coronary Syndrome in the Emergency Room. Artificial Intelligence in Medicine 2006, 38, 305–318, doi:10.1016/j.artmed.2006.07.006.

38. Ferretti, J.; Barbiero, P.; Randazzo, V.; Cirrincione, G.; Pasero, E. Towards Uncovering Feature Extraction from Temporal Signals in Deep CNN: The ECG Case Study. In Proceedings of the 2020 International Joint Conference on Neural Networks (IJCNN), Glasgow, UK, 2020, pp. 1-7, doi: 10.1109/IJCNN48605.2020.9207360 2020.

39. Cirrincione, G.; Randazzo, V.; Pasero, E. A Neural Based Comparative Analysis for Feature Extraction from ECG Signals. In Neural Approaches to Dynamics of Signal Exchanges; Esposito, A., Faundez-Zanuy, M., Morabito, F.C., Pasero, E., Eds.; Smart Innovation, Systems and Technologies; Springer: Singapore, 2020; pp. 247–256 ISBN 9789811389504.

40. Postema, P.G.; Wilde, A.A.M. The Measurement of the QT Interval. Current Cardiology Reviews 2014, 10, 287–294, doi:10.2174/1573403X10666140514103612.

41. Gaita, F.; Giustetto, C.; Bianchi, F.; Schimpf, R.; Haissaguerre, M.; Calò, L.; Brugada, R.; Antzelevitch, C.; Borggrefe, M.; Wolpert, C. Short QT Syndrome: Pharmacological Treatment. Journal of the American College of Cardiology 2004, 43, 1494–1499, doi:10.1016/j.jacc.2004.02.034.

42. Zhang, Z. A Gentle Introduction to Artificial Neural Networks. Annals of Translational Medicine 2016, 4, 370, doi:10.21037/atm.2016.06.20.

43. Bishop, C. M.; Nasser M. N., Pattern Recognition And Machine Learning, Vol. 4. No. 4. New York: Springer, 2006.

44. Goodfellow, I.; Bengio, Y.; Courville, A. Back-Propagation and Other Differentiation Algorithms. Deep Learning, MIT Press, 2016, 200–220.

45. Randazzo, V.; Puleo, E.; Paviglianiti, A.; Vallan, A.; Pasero, E. Development and Validation of an Algorithm for the Digitization of ECG Paper Images. Sensors 2022, 22, 7138. https://doi.org/10.3390/s22197138

46. Y. LeCun et al., Backpropagation Applied to Handwritten Zip Code Recognition. Neural Computation, vol. 1, no. 4, pp. 541-551, Dec. 1989, doi: 10.1162/neco.1989.1.4.541.

47. Tan, M., Le, Q.V., EfficientNetV2: Smaller Models and Fast Training. 2021, https://doi.org/10.48550/arXiv.2104.00298

48. Howard, A., Sandler et al., Searching for MobileNetV3. 2019, https://doi.org/10.48550/arXiv.1905.02244

49. Liu, Z., Mao, H., et al., A ConvNet for the 2020s. 2022, https://doi.org/10.48550/arXiv.2201.03545

50. Vaswani, A.; Shazeer, N.; Parmar, N.; Uszkoreit, J.; Jones, L.; Gomez, A.N.; Kaiser, L.; Polosukhin, I. Attention Is All You Need. 2017, doi:10.48550/ARXIV.1706.03762.

51. Dosovitskiy, A.; Beyer, L.; Kolesnikov, A.; Weissenborn, D.; Zhai, X.; Unterthiner, T.; Dehghani, M.; Minderer, M.; Heigold, G.; Gelly, S.; et al. An Image Is Worth 16x16 Words: Transformers for Image Recognition at Scale. 2020, doi:10.48550/ARXIV.2010.11929.

52. Bahdanau, D.; Cho, K.; Bengio, Y. Neural Machine Translation by Jointly Learning to Align and Translate. 2014, doi:10.48550/ARXIV.1409.0473.

53. Liu, Z., Cao, Y., Hu, H., et al., Swin Transformer: Hierarchical Vision Transformer using Shifted Windows. 2021, https://doi.org/10.48550/arXiv.2103.14030

54. J. Deng, W. Dong, R. Socher, L. -J. Li, Kai Li and Li Fei-Fei, ImageNet: A large-scale hierarchical image database. In Proceedings of the 2009 IEEE Conference on Computer Vision and Pattern Recognition, Miami, FL, USA, 2009, pp. 248-255, doi: 10.1109/CVPR.2009.5206848.

55. Sabour, S., Frosst, N., Hinton, G.E., Dynamic Routing Between Capsules. 2017, https://doi.org/10.48550/arXiv.1710.09829

56. Tolles J, Meurer WJ. Logistic Regression: Relating Patient Characteristics to Outcomes. JAMA 2016 Aug 2, 316, 533-4. doi: 10.1001/jama.2016.7653. PMID: 27483067.

57. Cubuk, E.D.; Zoph, B.; Shlens, J.; Le, Q.V. RandAugment: Practical Automated Data Augmentation with a Reduced Search Space. 2019, doi:10.48550/ARXIV.1909.13719.

58. Priori, S.G.; Blomström-Lundqvist, C.; Mazzanti, A.; Blom, N.; Borggrefe, M.; Camm, J.; Elliott, P.M.; Fitzsimons, D.; Hatala, R.; Hindricks, G.; et al. 2015 ESC Guidelines for the Management of Patients with Ventricular Arrhythmias and the Prevention of Sudden Cardiac Death: The Task Force for the Management of Patients with Ventricular Arrhythmias and the Prevention of Sudden

Cardiac Death of the European Society of Cardiology (ESC)Endorsed by: Association for European Paediatric and Congenital Cardiology (AEPC). European Heart Journal 2015, 36, 2793–2867, doi:10.1093/eurheartj/ehv316.

59. Schimpf, R.; Wolpert, C.; Bianchi, F.; Giustetto, C.; Gaita, F.; Bauersfeld, U.; Borggrefe, M. Congenital Short QT Syndrome and Implantable Cardioverter Defibrillator Treatment. Journal of Cardiovascular Electrophysiology 2003, 14, 1273–1277, doi:10.1046/j.1540-8167.2003.03278.x.

60. El-Battrawy, I.; Besler, J.; Ansari, U.; Liebe, V.; Schimpf, R.; Tülümen, E.; Rudic, B.; Lang, S.; Odening, K.; Cyganek, L.; et al. Long-Term Follow-up of Implantable Cardioverter-Defibrillators in Short QT Syndrome. Clinical Research in Cardiology 2019, 108, 1140–1146, doi:10.1007/s00392-019-01449-3.

61. LaValley, Michael P. Logistic regression. Circulation 2008, 117, pp 2395-2399, https://doi.org/10.1161/circulationaha.106.682658.

62. Randazzo, V.; Marchetti, G.; Giustetto, C.; Gugliermina, E.; Kumar, R.; Cirrincione, G.; ... & Pasero, E. Learning-Based Approach to Predict Fatal Events in Brugada Syndrome. In Applications of Artificial Intelligence and Neural Systems to Data Science 2023, pp. 63-72, Springer Nature Singapore, https://doi.org/10.1007/978-981-99-3592-5_6.

63. Netsanet, S.; Zhang, J.; Zheng, D. Bagged Decision Trees Based Scheme of Microgrid Protection Using Windowed Fast Fourier and Wavelet Transforms. Electronics 2018, 7, 61. https://doi.org/10.3390/electronics7050061

64. Samet, H. K-Nearest Neighbor Finding Using MaxNearestDist. IEEE Transactions on Pattern Analysis and Machine Intelligence, vol. 30, no. 2, pp. 243-252, Feb. 2008, doi: 10.1109/TPAMI.2007.1182.

65. Randazzo, V., Cirrincione, G., Pasero, E. (2020). Shallow Neural Network for Biometrics from the ECG-WATCH. In: Huang, DS., Bevilacqua, V., Hussain, A. (eds) Intelligent Computing Theories and Application. ICIC 2020. Lecture Notes in Computer Science(), vol 12463. Springer, Cham. https://doi.org/10.1007/978-3-030-60799-9_22

66. Lovino, M.; Randazzo, V.; Ciravegna, G.; Barbiero, P.; Ficarra, E.; Cirrincione, G. A survey on data integration for multi-omics sample clustering. Neurocomputing 2022, 488, pp 494-508, https://doi.org/10.1016/j.neucom.2021.11.094.